Influence of an electric field on the spin polarization in semiconductor superlattices

2005 J. Phys.: Condens. Matter 17 3865

(http://iopscience.iop.org/0953-8984/17/25/013)

INSTITUTE OF PHYSICS PUBLISHING JOURNAL OF PHYSICS: CONDENSED MATTER

J. Phys.: Condens. Matter **17** (2005) 3865–3877 doi:10.1088/0953-8984/17/25/013

Influence of an electric field on the spin polarization in semiconductor superlattices

P Kleinert[1] **and V V Bryksin**[2]

[1] Paul-Drude-Institut für Festkörperelektronik, Hausvogteiplatz 5-7, 10117 Berlin, Germany
[2] Physical Technical Institute, Politekhnicheskaya 26, 194021 St Petersburg, Russia

E-mail: kl@pdi-berlin.de

Received 23 March 2005, in final form 18 May 2005
Published 10 June 2005
Online at stacks.iop.org/JPhysCM/17/3865

Abstract

The influence of a quantizing electric field on the spin polarization is treated for semiconductor superlattices with a Rashba spin–orbit interaction. For weakly coupled superlattices, the quantum kinetic equation for the canonically transformed density matrix is analytically solved. The spin polarization, which is induced by a magnetic field via the Zeeman splitting, exhibits a sharp minimum at the cyclotron-Stark tunnelling resonance. This electric-field-induced resonant tunnelling mixes different spin states and leads to a strong spin depolarization.

1. Introduction

The emerging field of spintronics [1] has stimulated the study of spin–orbit interactions in low-dimensional semiconductor heterostructures. In this field, phenomena are under discussion that allow manipulations of the electronic spin. Many researchers have focused on the creation of spin-polarized carrier distributions in semiconductors, either optically [2] or by electrical injection from magnetic materials [3]. In addition, the electrical control of spins is of special interest, as it has great potential in semiconductor spintronic applications [1, 4, 5]. The spin–orbit interaction allows the generation of polarized spins and spin currents by applying a constant electric field. This extrinsic [6] and intrinsic [7] spin Hall effect can be used for spin injection in paramagnetic semiconductors. Most studies in this field are based on the semiclassical diffusive transport model [8, 9] and the linear response regime. Despite this exciting progress, there are only a few discussions of nonlinear spin phenomena under nonequilibrium conditions. In this paper, we fill this gap by theoretically treating the quantum transport regime at strong electric fields, when Wannier–Stark (WS) localization occurs and when field-induced resonant tunnelling between localized spin-up and spin-down states becomes possible. In a two-dimensional Rashba semiconductor superlattice, the large lattice constant along the superlattice axis gives rise to a large Bloch frequency Ω and related high-field effects of nonequilibrium carriers. The Zeeman splitting due to a perpendicular

magnetic field provides an energy gap between the spin-dependent WS states as well as an associated magnetization. Due to the field-induced tunnelling between spin-up and spin-down states, we observe a sharp minimum in the spin polarization at cyclotron-Stark resonances. This electric-field-controlled spin depolarization is treated within the density-matrix approach based on the WS representation.

2. The Hamiltonian

Let us consider a tight-binding model for electrons and their spins moving in the x–y plane of a two-dimensional semiconductor superlattice with the lattice period d along the x axis. The carriers are subject to a Rashba spin–orbit interaction and a spin splitting due to the Zeeman term of a constant magnetic field H oriented perpendicular to the plane. In the quasi-momentum representation, the Hamiltonian has the form

$$H_0 = \sum_{\mathbf{k},\sigma} \varepsilon_\sigma(\mathbf{k}) a^\dagger_{\mathbf{k}\sigma} a_{\mathbf{k}\sigma} + \sum_{\mathbf{k}} \sum_{\sigma,\sigma'} J_{\sigma\sigma'}(\mathbf{k}) a^\dagger_{\mathbf{k}\sigma} a_{\mathbf{k}\sigma'} - \mathrm{i}e\mathcal{E} \sum_{\mathbf{k},\sigma} \nabla_\kappa (a^\dagger_{\mathbf{k}-\frac{\kappa}{2}\sigma} a_{\mathbf{k}+\frac{\kappa}{2}\sigma})|_{\kappa=0}, \tag{1}$$

where the field operator $a^\dagger_{\mathbf{k}}$ [$a_{\mathbf{k}}$] creates [annihilates] an electron with quasi-momentum $\mathbf{k} = (k_x, k_y)$ and spin σ. The tight-binding dispersion relation of the two-dimensional superlattice is given by

$$\varepsilon_{1,2}(\mathbf{k}) = \varepsilon(\mathbf{k}) \mp \mu_\mathrm{B} H, \qquad \varepsilon(\mathbf{k}) = \frac{\Delta}{2}[1 - \cos(k_x d)] + \varepsilon(k_y), \tag{2}$$

where Δ and μ_B denote the width of the lowest miniband and the Bohr magneton, respectively. The kinetic energy of electrons moving in the y direction is given by $\varepsilon(k_y) = \hbar^2 k_y^2/(2m^*)$, with m^* being the effective mass. In equation (1), $\mathcal{E}$ denotes the electric field applied parallel to the x axis. The Rashba spin–orbit coupling matrix has the usual form

$$J_{\sigma\sigma'}(\mathbf{k}) = \begin{pmatrix} 0 & J(\mathbf{k}) \\ J^*(\mathbf{k}) & 0 \end{pmatrix}, \qquad J(\mathbf{k}) = \alpha m^* (\mathrm{i}v_x(\mathbf{k}) + v_y(\mathbf{k})), \tag{3}$$

with α being the Rashba coupling parameter and $v_j(\mathbf{k}) = \partial\varepsilon(\mathbf{k})/\partial\hbar k_j$. To diagonalize the Hamiltonian H_0, we apply a canonical transformation

$$a^\dagger_{\mathbf{k}1} = \Gamma_1(\mathbf{k}) c^\dagger_1(\mathbf{k}) - \Gamma^*_2(\mathbf{k}) c^\dagger_2(\mathbf{k}), \tag{4}$$

$$a^\dagger_{\mathbf{k}2} = \Gamma_2(\mathbf{k}) c^\dagger_1(\mathbf{k}) + \Gamma^*_1(\mathbf{k}) c^\dagger_2(\mathbf{k}), \tag{5}$$

and determine the unknown functions $\Gamma_{1,2}(\mathbf{k})$, which satisfy the normalization and periodic boundary conditions

$$|\Gamma_1(\mathbf{k})|^2 + |\Gamma_2(\mathbf{k})|^2 = 1, \qquad \Gamma_{1,2}(k_x + 2\pi/d, k_y) = \Gamma_{1,2}(k_x, k_y). \tag{6}$$

Assuming that the functions $\Gamma_{1,2}(\mathbf{k})$ solve the nonlinear differential equation

$$\Gamma_1\Gamma_2(\varepsilon_2(\mathbf{k}) - \varepsilon_1(\mathbf{k})) + J(\mathbf{k})\Gamma_1^2 - J^*(\mathbf{k})\Gamma_2^2 + \mathrm{i}e\mathcal{E}\left(\Gamma_1 \frac{\partial\Gamma_2}{\partial k_x} - \Gamma_2 \frac{\partial\Gamma_1}{\partial k_x}\right) = 0, \tag{7}$$

the transformed Hamiltonian can be written in the form

$$H_0 = \sum_{\mathbf{k},\mu} \left[E_\mu(\mathbf{k}) c^\dagger_\mu(\mathbf{k}) c_\mu(\mathbf{k}) + \mathrm{i}e\mathcal{E} \nabla_\kappa c^\dagger_\mu\left(\mathbf{k} + \frac{\kappa}{2}\right) c_\mu\left(\mathbf{k} - \frac{\kappa}{2}\right)\Big|_{\kappa=0} \right], \tag{8}$$

with the eigenenergies

$$E_{1,2} = \varepsilon_1|\Gamma_{1,2}|^2 + \varepsilon_2|\Gamma_{2,1}|^2 \pm J\Gamma_1\Gamma_2^* \pm J^*\Gamma_1^*\Gamma_2 - \mathrm{i}e\mathcal{E}\left(\Gamma_1 \frac{\partial\Gamma_1^*}{\partial k_x} + \Gamma_2 \frac{\partial\Gamma_2^*}{\partial k_x}\right). \tag{9}$$

To proceed, we shall conveniently express equation (7) by the following equivalent set of two linear differential equations [10, 11]

$$\mathrm{i}e\mathcal{E}\frac{\partial\Gamma_1(\mathbf{k})}{\partial k_x} = [\xi(k_x,k_y)+\mu_\mathrm{B}H]\Gamma_1(\mathbf{k}) - J^*(\mathbf{k})\Gamma_2(\mathbf{k}), \tag{10}$$

$$\mathrm{i}e\mathcal{E}\frac{\partial\Gamma_2(\mathbf{k})}{\partial k_x} = [\xi(k_x,k_y)-\mu_\mathrm{B}H]\Gamma_2(\mathbf{k}) - J(\mathbf{k})\Gamma_1(\mathbf{k}), \tag{11}$$

in which $\xi(\mathbf{k})$ is expressed by the equation

$$E_{1,2}(\mathbf{k}) = \varepsilon(\mathbf{k}) \pm \xi(\mathbf{k}). \tag{12}$$

A suitable scheme that allows a straightforward analytical approximation and a numerical solution of the boundary value problem in equations (10) and (11) is given in appendix A.

The diagonalization of the Hamiltonian H_0 is completed by applying a second transformation

$$c_\mu(\mathbf{k}) = \frac{1}{\sqrt{N_x}}\sum_m c_{m\mu}(k_y)\mathrm{e}^{-\mathrm{i}mk_xd-\mathrm{i}\chi_\mu(\mathbf{k})}, \tag{13}$$

with

$$\chi_\mu(\mathbf{k}) = \frac{1}{e\mathcal{E}}\int_0^{k_x}\mathrm{d}k_x'\,[E_\mu(k_x',k_y)-\langle E_\mu(\mathbf{k})\rangle], \tag{14}$$

and

$$\langle E_\mu(\mathbf{k})\rangle = \frac{d}{2\pi}\int_0^{2\pi/d}\mathrm{d}k_x\,E_\mu(k_x,k_y). \tag{15}$$

After this two-step procedure, we arrive at a Hamiltonian H_0 that becomes diagonal

$$H_0 = \sum_{m,\mu}\sum_{k_y}\varepsilon_{m\mu}(k_y)c^\dagger_{m\mu}(k_y)c_{m\mu}(k_y), \tag{16}$$

with the exact eigenenergies

$$\varepsilon_{m\mu}(k_y) = \langle E_\mu(\mathbf{k})\rangle - m\hbar\Omega. \tag{17}$$

Our basic Hamiltonian H_0 in equation (16) depends on the electric and magnetic field as well as on the Rashba spin–orbit coupling. We point out that the WS representation of H_0 in equation (16) is exactly equivalent to the original Hamiltonian in equation (1) expressed in the quasi-momentum representation. Therefore, the outlined schema allows an exact calculation of eigenenergies and eigenstates of our model Hamiltonian in equation (1) independent of the values for the Rashba coupling strength α, the magnetic field H, the electric field $\mathcal{E}$, or the miniband width Δ. To calculate the eigenenergies of H_0 from equation (17), we introduce dimensionless parameters

$$\tilde{\xi}(\mathbf{k}) = \frac{\xi(\mathbf{k})}{\hbar\Omega}, \qquad \epsilon = \frac{\mu_\mathrm{B}H}{\hbar\Omega}, \tag{18}$$

and determine $\tilde{\xi}$ from equation (A.9) in appendix A by taking into account that within the reduced zone scheme the energy contribution of the lateral electron motion is restricted by the inequalities

$$0 \leqslant \tilde{\xi}(k_y) \leqslant 1/2, \qquad \text{with } \tilde{\xi}(k_y) = \frac{d}{2\pi}\int_0^{2\pi/d}\mathrm{d}k_x\,\tilde{\xi}(k_x,k_y). \tag{19}$$

Figure 1 shows a numerical example for the energy parameter $\tilde{\xi}(k_y)$ as a function of k_yd (thick solid line) together with other branches, which correspond to other eigenenergies according to equation (17). Coupling between the quantum wells of the superlattice leads to anticrossings at

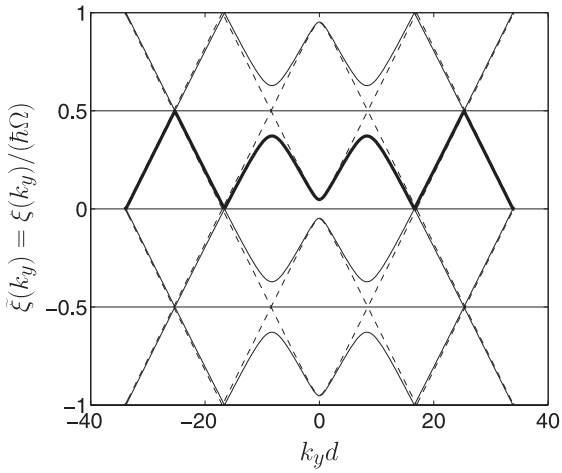

Figure 1. $\tilde{\xi}(k_y) = \xi(k_y)/(\hbar\Omega)$ as a function of $k_y d$ (thick solid line) for $\mathcal{E} = 17$ kV cm^{-1}, $d = 10$ nm, $\Delta = 100$ meV, $\alpha = 10^{-9}$ eV cm and $H = 1$ T. From bottom to top, the thin solid lines refer to $\tilde{\xi}(k_y) - 1$, $-\tilde{\xi}(k_y)$, and $-\tilde{\xi}(k_y) + 1$. The dashed lines are calculated for $\Delta = 0$.

field strengths, at which resonant tunnelling occurs. This effect is most pronounced for strongly coupled superlattices ($\Delta = 100$ meV in figure 1). If the quantum wells of the superlattice are completely decoupled ($\Delta = 0$), we obtain the analytical solution $\tilde{\xi}(k_y) = \kappa(k_y) + n_0$ and $\tilde{\xi}(k_y) = -\kappa(k_y) + n_0$ with $\kappa(k_y) = \sqrt{\epsilon^2 + \lambda^2(k_y)}$ and n_0 being any integer ($\lambda(k_y)$ is defined in appendix A by equation (A.1)). Obviously, this simple solution, which is shown by the dashed lines in figure 1, is only a poor approximation for tunnelling in superlattices with a large miniband width. The discrepancy between the exact solution (solid lines) and the simple approximation (dashed lines) is most pronounced at the anticrossings located at $k_y d = \pm 8.5$. For the description of these tunnelling transitions, the improved analytical solution derived in equation (A.13) (appendix A) is more appropriate. In the interval between the minima at $k_y d = -17$ and +17, equation (A.13) provides an accurate approximation for the energy splitting $\tilde{\xi}(k_y)$. For weakly coupled superlattices, however, the above simple analytical solution for $\Delta = 0$ is extremely useful. An example is shown in figure 2 for $\Delta = 10$ meV. In this case, only minor gaps appear at the anticrossings. The simple analytical approximation and the numerical result almost agree with each other. The main tunnelling resonance appears at $k_y = 0$, when the Bloch frequency Ω matches the cyclotron frequency ω_c ($\Omega = \omega_c$). Other resonances are of minor importance for weakly coupled superlattices.

3. Quantum kinetic equation

Quantum transport and field-induced carrier and spin redistribution in a nonequilibrium system are described by the density matrix

$$f_\sigma^{\sigma'}(\mathbf{k}, \mathbf{k}'|t) = \langle a^\dagger_{\mathbf{k}\sigma} a_{\mathbf{k}\sigma'} \rangle_t, \tag{20}$$

or its equivalent canonically transformed version

$$F_\mu^{\mu'}(\mathbf{k}, \mathbf{k}'|t) = \langle c^\dagger_\mu(\mathbf{k}) c_{\mu'}(\mathbf{k}') \rangle_t. \tag{21}$$

Most interesting is the density matrix in the WS representation, which diagonalizes the Hamiltonian H_0. Making use of the replacements $\mathbf{k} \to \mathbf{k} + \boldsymbol{\kappa}/2$ and $\mathbf{k}' \to \mathbf{k} - \boldsymbol{\kappa}/2$, we

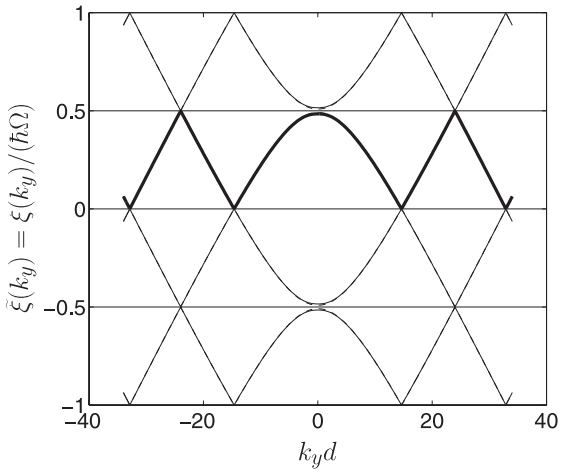

Figure 2. $\tilde{\xi}(k_y) = \xi(k_y)/(\hbar\Omega)$ as a function of $k_y d$ (thick solid line) for $\mathcal{E} = 17$ kV cm^{-1}, $d = 10$ nm, $\Delta = 10$ meV, $\alpha = 10^{-9}$ eV cm and $H = 10$ T. From bottom to top, the thin solid lines refer to $\tilde{\xi}(k_y) - 1$, $-\tilde{\xi}(k_y)$, and $-\tilde{\xi}(k_y) + 1$. The dashed lines are calculated for $\Delta = 0$.

introduce the functions

$$F_{\mu m}^{\mu' m'}(k_y, \kappa_y|t) = \left\langle c_{m\mu}^{\dagger}\left(k_y + \frac{\kappa_y}{2}\right) c_{m'\mu'}\left(k_y - \frac{\kappa_y}{2}\right)\right\rangle_t, \tag{22}$$

and obtain from equations (13) and (21)

$$F_{\mu}^{\mu'}(\mathbf{k}, \boldsymbol{\kappa}|t) = \mathrm{e}^{\mathrm{i}\chi_\mu(\mathbf{k}+\boldsymbol{\kappa}/2) - \mathrm{i}\chi_{\mu'}(\mathbf{k}-\boldsymbol{\kappa}/2)} \frac{1}{N_x} \sum_{m,m'} \mathrm{e}^{\mathrm{i}(m-m')k_x d + \mathrm{i}\kappa_x (m+m')/2} F_{\mu m}^{\mu' m'}(k_y, \kappa_y|t). \tag{23}$$

We treat an infinite periodic superlattice structure, for which κ_y enters the equations only as a parameter. Introducing the vector basis for the density matrix

$$f = f_1^1 + f_2^2, \qquad f_z = f_1^1 - f_2^2, \qquad f_x = f_2^1 + f_1^2, \qquad f_y = \mathrm{i}(f_2^1 - f_1^2), \tag{24}$$

(and similar definitions for $F_{\mu}^{\mu'}(\mathbf{k}|t)$ and $F_{\mu m}^{\mu' m'}(k_y|t)$), we obtain from equations (4), (5) and (13) the following relationship between $f_z(\mathbf{k})$ expressed by the original Hamiltonian H_0 in equation (1), and the elements of the density matrix in the WS representation

$$\begin{aligned} f_z(\mathbf{k}) = \frac{1}{N_x} \sum_{m,m'} \mathrm{e}^{\mathrm{i}(m-m')k_x d} \big\{ &\left(|\Gamma_1(\mathbf{k})|^2 - |\Gamma_2(\mathbf{k})|^2\right) F_z(m'-m, k_y) \\ &- 2\,\mathrm{Re}(\Gamma_1(\mathbf{k})\Gamma_2(\mathbf{k})\mathrm{e}^{\mathrm{i}\chi_{12}(\mathbf{k})}) F_x(m'-m, k_y) \\ &+ 2\,\mathrm{Im}(\Gamma_1(\mathbf{k})\Gamma_2(\mathbf{k})\mathrm{e}^{\mathrm{i}\chi_{12}(\mathbf{k})}) F_y(m'-m, k_y) \big\}, \end{aligned} \tag{25}$$

with $\chi_{12}(\mathbf{k}) = \chi_1(\mathbf{k}) - \chi_2(\mathbf{k})$.

A consistent treatment of high-field effects requires the inclusion of at least one inelastic scattering mechanism, by which the energy supplied by the electric field can dissipate. Let us treat scattering on polar-optical phonons, which is expressed by the Hamiltonian

$$H_{\mathrm{el-ph}} = \sum_{\mathbf{k},\sigma} \sum_{\mathbf{q},\mathbf{G}} g_\sigma(\mathbf{q} + \mathbf{G}) a_{\mathbf{k}+\mathbf{q}\sigma}^{\dagger} a_{\mathbf{k}\sigma} [b_{\mathbf{q}+\mathbf{G}} + b_{-\mathbf{q}-\mathbf{G}}^{\dagger}], \tag{26}$$

with $b_{\mathbf{q}}^{\dagger}$ and $b_{\mathbf{q}}$ denoting phonon creation and annihilation operators, respectively. The components of the phonon wavevector are restricted to the first Brillouin zone ($0 \leqslant q_{x,y} \leqslant 2\pi/d$). For the reciprocal lattice vector, we have $G_{x,y} = 2\pi m/d$, with $m = 0, 1, \ldots M$ and

$M = \mathrm{int}(d/a)$ (a is the lattice constant of the bulk system). In general, the coupling constant g_σ depends on the spin index. Applying the canonical transformation, the Hamiltonian for the electron–phonon interaction takes the form

$$H_{\mathrm{el-ph}} = \sum_{\mathbf{k},\mathbf{k}'} \sum_{G} \sum_{\mu\mu'} \Lambda_{\mu'\mu}(\mathbf{k}', \mathbf{k}) c^\dagger_{\mu'}(\mathbf{k}') c_\mu(\mathbf{k}) [b_{\mathbf{k}'-\mathbf{k}+\mathbf{G}} + b^\dagger_{-\mathbf{k}'+\mathbf{k}-\mathbf{G}}], \tag{27}$$

with the renormalized coupling

$$\Lambda_{\mu'\mu}(\mathbf{k}', \mathbf{k}) = \sum_\sigma g_\sigma(\mathbf{k}' - \mathbf{k} + \mathbf{G}) \mathbf{\Gamma}^\sigma_{\mu'\mu}(\mathbf{k}', \mathbf{k}), \tag{28}$$

and

$$\mathbf{\Gamma}^1_{\mu'\mu}(\mathbf{k}', \mathbf{k}) = \begin{pmatrix} \Gamma_1(\mathbf{k}')\Gamma_1^*(\mathbf{k}) & -\Gamma_1(\mathbf{k}')\Gamma_2(\mathbf{k}) \\ -\Gamma_2^*(\mathbf{k}')\Gamma_1^*(\mathbf{k}) & \Gamma_2^*(\mathbf{k}')\Gamma_2(\mathbf{k}) \end{pmatrix}, \tag{29}$$

$$\mathbf{\Gamma}^2_{\mu'\mu}(\mathbf{k}', \mathbf{k}) = \begin{pmatrix} \Gamma_2(\mathbf{k}')\Gamma_2^*(\mathbf{k}) & \Gamma_2(\mathbf{k}')\Gamma_1(\mathbf{k}) \\ \Gamma_1^*(\mathbf{k}')\Gamma_2^*(\mathbf{k}) & \Gamma_1^*(\mathbf{k}')\Gamma_1(\mathbf{k}) \end{pmatrix}. \tag{30}$$

Our final result for $H_{\mathrm{el-ph}}$ is obtained by applying the second transformation according to equation (13). In this WS representation, the interaction Hamiltonian is given by

$$H_{\mathrm{el-ph}} = \sum_{\mathbf{k},\mathbf{k}'} \sum_{G} \sum_{\mu\mu'} \sum_{m,m'} \Lambda_{m'\mu',m\mu}(\mathbf{k}', \mathbf{k}) c^\dagger_{m'\mu'}(k'_y) c_{m\mu}(k_y) [b_{\mathbf{k}'-\mathbf{k}+\mathbf{G}} + b^\dagger_{-\mathbf{k}'+\mathbf{k}-\mathbf{G}}], \tag{31}$$

with the matrix elements

$$\Lambda_{m'\mu',m\mu}(\mathbf{k}', \mathbf{k}) = \Lambda_{\mu'\mu}(\mathbf{k}', \mathbf{k}) \mathrm{e}^{\mathrm{i}m'k'_x d - \mathrm{i}mk_x d + \mathrm{i}\chi_{\mu'}(\mathbf{k}') - \mathrm{i}\chi_\mu(\mathbf{k})}. \tag{32}$$

The quantum kinetic equation for the density matrix is obtained from the Liouville equation. We restrict the discussion to a nondegenerate electron gas, whose equilibrium statistics is described by the Boltzmann distribution function. Switching to Laplace space with respect to the time variable, we obtain our main result

$$\left\{ s - \frac{\mathrm{i}}{\hbar} [\varepsilon_{m\mu}(k_y) - \varepsilon_{m'\mu'}(k_y)] \right\} F^{\mu'm'}_{\mu m}(k_y|s) = \sum_{k'_y} \sum_{m_1,m_2} \sum_{\mu_1,\mu_2} F^{\mu_2 m_2}_{\mu_1 m_1}(k'_y|s) W^{m_2\mu_2,m'\mu'}_{m_1\mu_1,m\mu}(k'_y, k_y|s). \tag{33}$$

An explicit expression for the scattering rates W is given in appendix B. Let us treat this coupled set of equations in the vector basis. In the equations for F and F_z strongly oscillating scattering rates appear with three equal spin indices (e.g., $W^{m_2 1,m'1}_{m_1 1,m2}$ etc), which are proportional to the spin–orbit coupling constant α. Under the condition $\sqrt{2m^* k_\mathrm{B} T}\alpha/\hbar < \mu_\mathrm{B} H$, these contributions can be neglected, and we obtain a closed set of equations for the density-matrix components F and F_z. In addition to this approximation, let us focus on the high-field regime, when $\Omega\tau_{\mathrm{eff}} \gg 1$ is satisfied (τ_{eff} is an effective scattering time) so that the diagonal elements of the density matrix with respect to the layer index m dominate. In this case, the kinetic equations simplify considerably, and we obtain

$$\sum_{k'_y} F(0, k'_y) \sum_m [W^{m1,01}_{m1,01}(k'_y, k_y) + W^{m2,01}_{m2,01}(k'_y, k_y)] + \sum_{k'_y} F_z(0, k'_y) \sum_m [W^{m1,01}_{m1,01}(k'_y, k_y) - W^{m2,01}_{m2,01}(k'_y, k_y)] = 0, \tag{34}$$

$$\sum_{k'_y} F(0, k'_y) \sum_m [W^{m2,02}_{m2,02}(k'_y, k_y) + W^{m1,02}_{m1,02}(k'_y, k_y)] - \sum_{k'_y} F_z(0, k'_y) \sum_m [W^{m2,02}_{m2,02}(k'_y, k_y) - W^{m1,02}_{m1,02}(k'_y, k_y)] = 0, \tag{35}$$

which is quite similar to the kinetic equation for a double-quantum-well superlattice treated previously (see equation (39) in [12]). Inserting the explicit expression for the scattering rates from equation (B.1) into these equations and calculating the t integrals, which result in δ functions in the steady state ($s \to 0$), we obtain a kinetic equation that can be solved analytically in the weak coupling limit ($\Delta/\hbar\Omega \ll 1$), when the states are mainly localized in a given well (only $m = 0$). Details of the derivation are summarized in appendix C. The analytic solution of the kinetic equations is given by

$$F(m=0,k_y) = A\exp\left(-\frac{\varepsilon(k_y)}{k_\mathrm{B}T}\right)\cosh\left(\frac{\xi(k_y)-n_0(k_y)\hbar\Omega}{k_\mathrm{B}T}\right), \tag{36}$$

$$F_z(m=0,k_y) = -A\exp\left(-\frac{\varepsilon(k_y)}{k_\mathrm{B}T}\right)\sinh\left(\frac{\xi(k_y)-n_0(k_y)\hbar\Omega}{k_\mathrm{B}T}\right), \tag{37}$$

where the constant A is calculated from the normalization of the charge contribution

$$\sum_{k_y} F(m=0,k_y) = 1. \tag{38}$$

We conclude that thermal, Boltzmann-like lateral distribution functions $F_1^1(m=0,k_y)$ and $F_2^2(m=0,k_y)$ solve the kinetic equation under the condition of sequential tunnelling in the quantum limit at high electric fields.

4. Electric-field dependence of the spin polarization

A constant magnetic field applied perpendicular to the x–y plane results in an energy gap that separates different spin states. The resulting spin polarization is studied under high electric fields, when carriers are WS localized in the quantum wells of the superlattice and when a thermal lateral distribution function is set up in the quantum regime. For electric field strengths that satisfy the condition $n\Omega = m\omega_\mathrm{c}$ (m, n are integers), field-induced resonant tunnelling strongly mixes the spin states so that the spin polarization collapses. Below and above these particular electric field strengths, the magnetization recovers and approaches its value at $\mathcal{E} = 0$. This physical picture is confirmed by our quantum-kinetic approach. In the limit of weak electron–phonon coupling and quantizing electric fields ($\Omega\tau_\mathrm{eff} \gg 1$), we can neglect the oscillating contribution in the second line of equation (25) and obtain for the spin polarization

$$f_z = \sum_{\mathbf{k}}(f_1^1(\mathbf{k}) - f_2^2(\mathbf{k})) = \sum_{k_y} F_z(m=0,k_y)\sum_{k_x}(|\Gamma_1(\mathbf{k})|^2 - |\Gamma_2(\mathbf{k})|^2). \tag{39}$$

Using this result and equation (37), the electric-field dependence of the spin polarization is numerically calculated by using the exact results for $\xi(k_y)$ and $\Gamma_{1,2}(\mathbf{k})$ obtained from the procedure outlined in appendix A. Note that the solution in equation (37) is only applicable for weakly coupled superlattices. A numerical example for the electric-field dependence of the spin polarization is shown in figure 3 for superlattices with $\Delta = 2$ and 10 meV, respectively. In the absence of resonant tunnelling ($\Delta = 0$), the spin polarization is independent of the electric field and given by the value

$$f_z = \sum_{\mathbf{k}} f_z(\mathbf{k}) = \tanh\left(\frac{\mu_\mathrm{B}|H|}{k_\mathrm{B}T}\right), \tag{40}$$

which agrees with the result for $\mathcal{E} = 0$. The horizontal line in figure 3 displays this limiting value. With increasing miniband width Δ, a strong antiresonance develops in the spin polarization as a result of field-induced resonant tunnelling between different spin states.

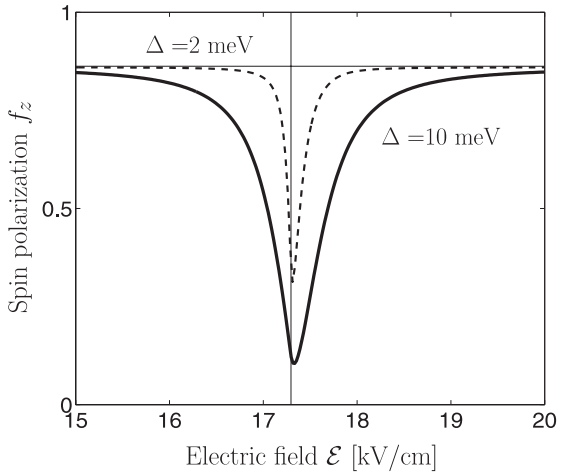

Figure 3. Spin polarization f_z as a function of the electric field for $\Delta = 2$ meV (dashed line) and $\Delta = 10$ meV (solid line) with $H = 10$ T, $T = 77$ K, $d = 10$ nm. The cyclotron-Stark resonance at $\Omega = \omega_c$ is marked by a thin vertical line.

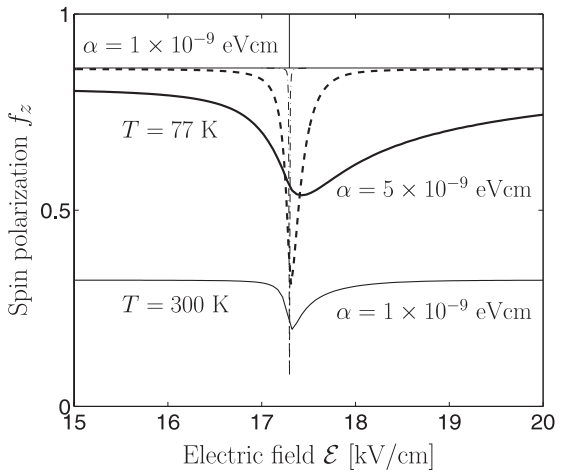

Figure 4. Spin polarization f_z as a function of the electric field for $H = 10$ T and $\Delta = 2$ meV. The thick solid (dashed) lines are calculated with $\alpha = 1$ (5) $\times 10^{-9}$ eV cm and $T = 77$ K. The dash–dotted line refers to a weak Rashba coupling of $\alpha = 0.05 \times 10^{-9}$ eV cm. Parameters for the thin solid line are $T = 300$ K and $\alpha = 10^{-9}$ eV cm.

Figure 3 shows the main antiresonance at $\Omega = \omega_c$. In general, we expect sharp minima in the spin polarization also for other cyclotron Stark resonances. The description of these weak antiresonances is not possible within the approximation in equations (36) and (37), but requires an improved solution of the kinetic equations by taking into account the Stark ladder. An analytical approach of this kind is proposed in appendix C.

The character of the antiresonances also depends on the value of the Rashba coupling constant α as shown in figure 4. The antiresonance exhibits a sharp δ-like line shape, when α approaches zero (an example is shown by the dash–dotted line). Consequently, the spin–orbit coupling plays a decisive role for the resolution of the predicted antiresonance in a real

experiment. With increasing α, the line shape of the antiresonance becomes asymmetric, with a shifted and broadened minimum (thick solid line). By increasing the lattice temperature (thin solid line), the field-induced spin depolarization at the tunnelling resonance appreciably decreases.

5. Summary

We provided a theoretical model to answer the question of whether the spin polarization of nonequilibrium carriers in a semiconductor can be controlled by a quantizing electric field. Weakly coupled superlattices were treated, in which the spin polarization is due to the Zeeman splitting. The application of a strong electric field along the superlattice axis leads to resonant tunnelling between different spin states. Due to this mixing of eigenstates at the electric-field-induced tunnelling resonance, a strong spin depolarization occurs, the strength of which depends on the miniband width, the Rashba spin–orbit coupling, and the lattice temperature. This collapse of the spin polarization appears in a narrow region of electric field strengths and is sufficiently strong that it might be of interest for spintronic applications.

The physical mechanism leading to spin depolarization due to field-induced tunnelling resonances is expected to exist also in layered three-dimensional superlattices with Dresselhaus spin–orbit coupling, for which the experimental detection of the predicted antiresonance in the spin polarization is much easier than in the considered two-dimensional electron gas with a superlattice structure. Furthermore, in our model, the spin polarization is due to the Zeeman splitting induced by a strong magnetic field. For device applications, it seems to be more appropriate to achieve a pronounced spin polarization by incorporating into the superlattice structure alternating ferromagnetic layers with a large internal magnetic field.

Acknowledgments

Discussions with M Ramsteiner and partial support by the Deutsche Forschungsgemeinschaft are gratefully acknowledged.

Appendix A. Solution of equations (10) and (11)

To solve the set of linear differential equations (10) and (11), we apply a calculational scheme that was outlined in [11]. Introducing dimensionless parameters

$$\lambda(k_y) = \frac{\alpha k_y}{\hbar\Omega}, \qquad \delta = \frac{\alpha m^* \Delta}{2\hbar^2 e\mathcal{E}}, \qquad x = k_x d, \tag{A.1}$$

the equations are expressed by

$$\mathrm{i}\frac{\partial \Gamma_1(x,k_y)}{\partial x} = (\tilde{\xi}(x,k_y)+\epsilon)\Gamma_1(x,k_y) - \lambda(k_y)\Gamma_2(x,k_y) + \mathrm{i}\delta\sin(x)\Gamma_2(x,k_y), \tag{A.2}$$

$$\mathrm{i}\frac{\partial \Gamma_2(x,k_y)}{\partial x} = (\tilde{\xi}(x,k_y)-\epsilon)\Gamma_2(x,k_y) - \lambda(k_y)\Gamma_1(x,k_y) - \mathrm{i}\delta\sin(x)\Gamma_1(x,k_y). \tag{A.3}$$

A solution is searched for in the form

$$\Gamma_1(x,k_y) = \frac{1}{\sqrt{2}}\exp\left(-\mathrm{i}\int_0^x \mathrm{d}x'\,\tilde{\xi}(x',k_y)\right) \times [F_1(f_1(x,k_y) - \mathrm{i}f_2(x,k_y)) - \mathrm{i}F_2(f_1(x,k_y)^* - \mathrm{i}f_2(x,k_y)^*)], \tag{A.4}$$

$$\Gamma_2(x,k_y)=\frac{1}{\sqrt{2}}\exp\left(-\mathrm{i}\int_0^x \mathrm{d}x'\,\tilde{\xi}(x',k_y)\right)$$
$$\times\left[F_1(f_2(x,k_y)-\mathrm{i}f_1(x,k_y))+\mathrm{i}F_2(f_2(x,k_y)^*-\mathrm{i}f_1(x,k_y)^*)\right], \tag{A.5}$$

with $|F_1|^2+|F_2|^2=1$ so that

$$|f_1(x,k_y)|^2+|f_2(x,k_y)|^2=1. \tag{A.6}$$

Inserting the ansatz for $\Gamma_{1,2}$ into equations (A.2) and (A.3), we obtain

$$\mathrm{i}\frac{\partial f_1(x,k_y)}{\partial x}=\delta\sin(x)f_1(x,k_y)-(\lambda(k_y)+\mathrm{i}\epsilon)f_2(x,k_y), \tag{A.7}$$

$$\mathrm{i}\frac{\partial f_2(x,k_y)}{\partial x}=-\delta\sin(x)f_2(x,k_y)-(\lambda(k_y)-\mathrm{i}\epsilon)f_1(x,k_y), \tag{A.8}$$

which has the form of coupled Schrödinger equations for the wavefunctions $f_{1,2}(x,k_y)$, for which we apply the 'initial' conditions $f_1(0,k_y)=1$ and $f_2(0,k_y)=0$. Due to the lattice periodicity, we have $\Gamma_{1,2}(0,k_y)=\Gamma_{1,2}(2\pi,k_y)$, which leads to the dispersion relation

$$\cos\left[\int_0^{2\pi}\mathrm{d}x'\,\tilde{\xi}(x',k_y)\right]=\mathrm{Re}\,f_1(2\pi,k_y), \tag{A.9}$$

and an equation from which $F_{1,2}$ can be calculated up to a undetermined phase factor.

Let us derive a simple analytical solution of equations (A.2) and (A.3) that is valid for $\epsilon<1/2$ and $\delta\ll 1$. In this case, we neglect the x dependence in $\tilde{\xi}(x,k_y)$ and perform a discrete Fourier transformation

$$\Gamma_\mu(x,k_y)=\sum_{n=-\infty}^{\infty}\mathrm{e}^{-\mathrm{i}nx}\Gamma_{\mu,n}(k_y). \tag{A.10}$$

The set of linear equations for the Fourier components

$$(\tilde{\xi}(k_y)+\epsilon-n)\Gamma_{1,n}(k_y)-\lambda(k_y)\Gamma_{2,n}(k_y)=-\frac{\delta}{2}(\Gamma_{2,n+1}(k_y)-\Gamma_{2,n-1}(k_y)), \tag{A.11}$$

$$(\tilde{\xi}(k_y)-\epsilon-n)\Gamma_{2,n}(k_y)-\lambda(k_y)\Gamma_{1,n}(k_y)=\frac{\delta}{2}(\Gamma_{1,n+1}(k_y)-\Gamma_{1,n-1}(k_y)), \tag{A.12}$$

is solved by focusing on the main tunnelling transitions described by $\Gamma_{1,0}$, $\Gamma_{1,1}$, $\Gamma_{2,0}$, and $\Gamma_{2,1}$. Equating the determinant of the respective 4×4 coefficient matrix to zero, we find the solution

$$\tilde{\xi}_{1,2}(k_y)=\tfrac{1}{2}\left(1\pm\sqrt{(2\kappa(k_y)-1)^2+\delta^2}\right), \tag{A.13}$$

which is applicable for $\epsilon<1/2$ and $\delta\ll 1$.

Appendix B. Scattering rates

The scattering rates in the kinetic equation (33) couple different spin and charge components of the density matrix to each other. The rates consist of scattering-in and scattering-out contributions given by

$$W^{m_2\mu_2,m'\mu'}_{m_1\mu_1,m\mu}(k_y',k_y|s)$$
$$=\frac{1}{\hbar^2}\sum_{q_x}\mathrm{e}^{\mathrm{i}(m_1-m_2)q_xd}\Pi_{\mu_1\mu}(k_y',k_y|q_x,m_1-m)\Pi^*_{\mu_2\mu'}(k_y',k_y|q_x,m_2-m')$$
$$\times\left\{\int_0^\infty\mathrm{d}t\exp\left[-st+\frac{\mathrm{i}t}{\hbar}(\varepsilon_{m_1\mu_1}(k_y')-\varepsilon_{m'\mu'}(k_y))\right][(N_0+1)\mathrm{e}^{-\mathrm{i}\omega_0t}+N_0\mathrm{e}^{\mathrm{i}\omega_0t}]\right.$$

$$
\begin{aligned}
&+\int_0^\infty \mathrm{d}t\,\exp\left[-st+\frac{\mathrm{i}t}{\hbar}(\varepsilon_{m\mu}(k_y)-\varepsilon_{m_2\mu_2}(k'_y))\right][(N_0+1)\mathrm{e}^{\mathrm{i}\omega_0 t}+N_0\mathrm{e}^{-\mathrm{i}\omega_0 t}]\Big\}\\
&-\frac{1}{\hbar^2}\delta_{m_2,m'}\delta_{\mu_2,\mu'}\delta_{k'_y,k_y}\\
&\times\sum_{\overline{m},\overline{\mu}}\sum_{\overline{k}_y}\sum_{q_x}\Pi_{\overline{\mu}\mu}(\overline{k}_y,k_y|q_x,\overline{m}-m)\Pi^*_{\overline{\mu}\mu_1}(\overline{k}_y,k_y|q_x,\overline{m}-m_1)\\
&\times\int_0^\infty \mathrm{d}t\,\exp\left[-st+\frac{\mathrm{i}t}{\hbar}(\varepsilon_{\overline{m\mu}}(\overline{k}_y)-\varepsilon_{m'\mu'}(k_y))\right][(N_0+1)\mathrm{e}^{\mathrm{i}\omega_0 t}+N_0\mathrm{e}^{-\mathrm{i}\omega_0 t}]\\
&-\frac{1}{\hbar^2}\delta_{m_1,m}\delta_{\mu_1,\mu}\delta_{k'_y,k_y}\\
&\times\sum_{\overline{m},\overline{\mu}}\sum_{\overline{k}_y}\sum_{q_x}\Pi_{\overline{\mu}\mu_2}(\overline{k}_y,k_y|q_x,\overline{m}-m_2)\Pi^*_{\overline{\mu}\mu'}(\overline{k}_y,k_y|q_x,\overline{m}-m')\\
&\times\int_0^\infty \mathrm{d}t\,\exp\left[-st+\frac{\mathrm{i}t}{\hbar}(\varepsilon_{m\mu}(k_y)-\varepsilon_{\overline{m\mu}}(\overline{k}_y))\right][(N_0+1)\mathrm{e}^{-\mathrm{i}\omega_0 t}+N_0\mathrm{e}^{\mathrm{i}\omega_0 t}],
\end{aligned}
\tag{B.1}
$$

with the matrix elements

$$
\Pi_{\mu'\mu}(k'_y,k_y|q_x,m)=\sum_{k_x}\mathrm{e}^{\mathrm{i}mk_xd+\mathrm{i}\chi_{\mu'}(k_x+q_x,k'_y)-\mathrm{i}\chi_\mu(k_x,k_y)}\Lambda_{\mu'\mu}(k_x+q_x,k'_y|k_x,k_y). \tag{B.2}
$$

Appendix C. Analytical solution of the kinetic equations

Let us treat the kinetic equations for a superlattice with a narrow miniband width ($\Delta/\hbar\Omega\ll 1$). With the notation

$$
\Phi_{\mu\mu'}(k'_y,k_y|m)=\sum_{q_x}|\Pi_{\mu\mu'}(k'_y,k_y|q_x,m)|^2, \tag{C.1}
$$

we obtain from the equations (34) and (B.1) the equation

$$
\begin{aligned}
&\sum_{k'_y}\sum_m\big\{\Phi_{11}(k'_y,k_y|m)\\
&\quad\times\big\{F_1^1(0,k'_y)[(N_0+1)\delta(\varepsilon_{k'_y}-\varepsilon_{k_y}-m\hbar\Omega-\hbar\omega_0)\\
&\quad+N_0\delta(\varepsilon_{k'_y}-\varepsilon_{k_y}-m\hbar\Omega+\hbar\omega_0)]\\
&\quad-F_1^1(0,k_y)[(N_0+1)\delta(\varepsilon_{k'_y}-\varepsilon_{k_y}-m\hbar\Omega+\hbar\omega_0)\\
&\quad+N_0\delta(\varepsilon_{k'_y}-\varepsilon_{k_y}-m\hbar\Omega-\hbar\omega_0)]\big\}\\
&\quad+\Phi_{21}(k'_y,k_y|m)\big\{F_2^2(0,k'_y)[(N_0+1)\delta(\varepsilon_{k'_y}-\varepsilon_{k_y}-m\hbar\Omega-2\xi(k'_y)-\hbar\omega_0)\\
&\quad+N_0\delta(\varepsilon_{k'_y}-\varepsilon_{k_y}-m\hbar\Omega-2\xi(k'_y)+\hbar\omega_0)]\\
&\quad-F_1^1(0,k_y)[(N_0+1)\delta(\varepsilon_{k'_y}-\varepsilon_{k_y}-m\hbar\Omega-2\xi(k'_y)+\hbar\omega_0)\\
&\quad+N_0\delta(\varepsilon_{k'_y}-\varepsilon_{k_y}-m\hbar\Omega-2\xi(k'_y)-\hbar\omega_0)]\big\}\big\}=0,
\end{aligned}
\tag{C.2}
$$

with $\varepsilon_{k_y}=\varepsilon(k_y)+\xi(k_y)$, which can be analytically solved for weakly coupled superlattices ($\Delta/\hbar\Omega\ll 1$). For $\Delta=0$, we obtain from equations (10) and (11): if $\tilde{\xi}(k_y)=-\kappa(k_y)+n_0(k_y)$ then

$$\Gamma_1(\mathbf{k}) = \sqrt{\frac{\kappa(k_y)+\epsilon}{2\kappa(k_y)}}\mathrm{e}^{-\mathrm{i}n_0(k_y)k_x d}, \qquad \Gamma_2(\mathbf{k}) = \sqrt{\frac{\kappa(k_y)-\epsilon}{2\kappa(k_y)}}\mathrm{e}^{-\mathrm{i}n_0(k_y)k_x d}, \tag{C.3}$$

so that $|\Gamma_1(\mathbf{k})|^2 - |\Gamma_2(\mathbf{k})|^2 = \epsilon/\kappa(k_y)$.
If $\tilde{\xi}(k_y) = \kappa(k_y) - n_0(k_y)$ then

$$\Gamma_1(\mathbf{k}) = \sqrt{\frac{\kappa(k_y)-\epsilon}{2\kappa(k_y)}}\mathrm{e}^{\mathrm{i}n_0(ky)k_x d}, \qquad \Gamma_2(\mathbf{k}) = \sqrt{\frac{\kappa(k_y)+\epsilon}{2\kappa(k_y)}}\mathrm{e}^{\mathrm{i}n_0(ky)k_x d}, \tag{C.4}$$

so that $|\Gamma_1(\mathbf{k})|^2 - |\Gamma_2(\mathbf{k})|^2 = -\epsilon/\kappa(k_y)$. Using this result, the matrix elements $\Phi_{\mu\mu'}$ can be calculated. For a constant coupling strength ($g_\sigma(\mathbf{q}) = g$), we obtain

$$\Phi_{11}(k'_y, k_y) = |g|^2\gamma_{11}(k'_y, k_y)F_{m+n_0(k_y)-n_0(k'_y)}\left(\frac{\Delta}{\hbar\Omega}\right), \tag{C.5}$$

$$\gamma_{11} = \frac{1}{2} \pm \frac{\epsilon^2}{2\kappa(k_y)\kappa(k'_y)} \qquad \begin{cases} \text{if } n_0(k_y) = n_0(k'_y) \\ \text{if } n_0(k_y) \neq n_0(k'_y) \end{cases} \tag{C.6}$$

$$\Phi_{21}(k'_y, k_y) = |g|^2\gamma_{21}(k'_y, k_y)F_{m+n_0(k_y)+n_0(k'_y)}\left(\frac{\Delta}{\hbar\Omega}\right), \tag{C.7}$$

$$\gamma_{21} = \frac{1}{2} \mp \frac{\epsilon^2}{2\kappa(k_y)\kappa(k'_y)} \qquad \begin{cases} \text{if } n_0(k_y) = n_0(k'_y) \\ \text{if } n_0(k_y) \neq n_0(k'_y) \end{cases}, \tag{C.8}$$

with the abbreviation

$$F_m(x) = \int_0^\pi \frac{\mathrm{d}t}{\pi} J_m^2(x\sin(t)). \tag{C.9}$$

J_m denotes the Bessel function. In the limit $\Delta \ll \hbar\Omega$, we have $\Phi_{11} \sim \delta_{m+n_0(k_y)-n_0(k'_y),0}$ and $\Phi_{21} \sim \delta_{m+n_0(k_y)+n_0(k'_y),0}$, which is used to derive the solution of equation (C.2)

$$F_1^1(0, k_y) = A\exp\left(-\frac{\tilde{\varepsilon}_1(k_y)}{k_\mathrm{B}T}\right), \qquad F_2^2(0, k_y) = A\exp\left(-\frac{\tilde{\varepsilon}_2(k_y)}{k_\mathrm{B}T}\right), \tag{C.10}$$

with

$$\tilde{\varepsilon}_{1,2}(k_y) = \varepsilon(k_y) \pm (\xi(k_y) - n_0(k_y)\hbar\Omega). \tag{C.11}$$

With this analytical result for the components of the density matrix, the electric-field dependence of the magnetization is calculated in section 4.

The thermal lateral distribution functions in equation (C.10) can be used to study spin depolarization at the main tunnelling resonance ($\Omega = \omega_\mathrm{c}$). However, to treat weak antiresonances of higher order ($n\Omega = m\omega_\mathrm{c}$), the WS ladder has to be retained in equation (C.2). For small spin–orbit coupling, we can apply a perturbation approach with respect to α. From equations (C.5) to (C.8), we obtain $\Phi_{11} \sim \alpha^0$, $\Phi_{21} \sim \alpha^2$ (and similarly $\Phi_{22} \sim \alpha^0$, $\Phi_{12} \sim \alpha^2$), which justifies the ansatz

$$F_1^1(0, k_y) = A_1\exp\left(-\frac{\tilde{\varepsilon}_1(k_y)}{k_\mathrm{B}T}\right), \qquad F_2^2(0, k_y) = A_2\exp\left(-\frac{\tilde{\varepsilon}_2(k_y)}{k_\mathrm{B}T}\right), \tag{C.12}$$

for weakly coupled superlattices. Inserting this result into the kinetic equation (C.2), we get

$$\begin{aligned}\sum_m \sum_{k_y,k'_y} F_m\left(\frac{\Delta}{\hbar\Omega}\right)\Big\{&A_1\gamma_{11}(k'_y, k_y)\mathrm{e}^{-\frac{\tilde{\varepsilon}_1(k_y)}{k_\mathrm{B}T}}(\mathrm{e}^{-\frac{m\hbar\Omega}{k_\mathrm{B}T}} - 1) \\ &\times \left[\delta(\tilde{\varepsilon}_1(k'_y) - \tilde{\varepsilon}_1(k_y) - m\hbar\Omega + \hbar\omega_0)\right. \\ &\left. + \mathrm{e}^{-\frac{\hbar\omega_0}{k_\mathrm{B}T}}\delta(\tilde{\varepsilon}_1(k'_y) - \tilde{\varepsilon}_1(k_y) + m\hbar\Omega - \hbar\omega_0)\right]\end{aligned}$$

$$+\gamma_{21}(k'_y,k_y)\mathrm{e}^{-\frac{\tilde{\varepsilon}_1(k_y)}{k_\mathrm{B}T}}(A_2\mathrm{e}^{-\frac{m\hbar\Omega}{k_\mathrm{B}T}}-A_1)$$
$$\times[\delta(\tilde{\varepsilon}_2(k'_y)-\tilde{\varepsilon}_1(k_y)-m\hbar\Omega+\hbar\omega_0)$$
$$+\mathrm{e}^{-\frac{\hbar\omega_0}{k_\mathrm{B}T}}\delta(\tilde{\varepsilon}_1(k'_y)-\tilde{\varepsilon}_1(k_y)+m\hbar\Omega-\hbar\omega_0)]\Big\}=0, \tag{C.13}$$

which can be used together with the normalization condition

$$\sum_{k_y}\left[A_1\exp\left(-\frac{\tilde{\varepsilon}_1(k_y)}{k_\mathrm{B}T}\right)+A_2\exp\left(-\frac{\tilde{\varepsilon}_2(k_y)}{k_\mathrm{B}T}\right)\right]=1, \tag{C.14}$$

to calculate the quantities A_1 and A_2, in which the complete Stark ladder enters. This approximation can be used to treat the spin depolarization at higher-order cyclotron-Stark resonances.

References

[1] Wolf S A, Awschalom D D, Buhrman R A, Daughton J M, von Molnar S, Roukes M L, Chtchelkanova A Y and Treger D M 2001 *Science* **294** 1488
[2] Kikkawa J M and Awschalom D D 1998 *Phys. Rev. Lett.* **80** 4313
[3] Fiederling R, Keim M, Reuscher G, Ossau W, Schmidt G, Waag A and Mohlenkamp L W 1999 *Nature* **402** 787
[4] Datta S and Das B 1990 *Appl. Phys. Lett.* **56** 665
[5] Prinz G A 1998 *Science* **282** 1660
[6] Hirsch J E 1999 *Phys. Rev. Lett.* **83** 1834
[7] Murakami S, Nagaosa N and Zhang S C 2003 *Science* **301** 1348
[8] Qi Y and Zhang Z 2003 *Phys. Rev.* B **67** 052407
[9] Burkov A A, Nunez A S and MacDonald A H 2004 *Phys. Rev.* B **70** 155308
[10] Bryksin V V, de Dios M and Firsov Y A 1987 *Fiz. Tverd. Tela* **29** 1141
Bryksin V V, de Dios M and Firsov Y A 1987 *Sov. Phys.—Solid State* **29** 651 (Engl. Transl.)
[11] Bryksin V V 1987 *Fiz. Tverd. Tela* **29** 2027
Bryksin V V 1987 *Sov. Phys.—Solid State* **29** 1166 (Engl. Transl.)
[12] Kleinert P, Schrottke L, Grahn H T and Bryksin V V 2003 *Phys. Rev.* B **67** 195306